Journal of Materials Chemistry B

Accepted Manuscript

This article can be cited before page numbers have been issued, to do this please use: J. Liu, X. Wang, G. Lu, J. Z. Tang, Y. Wang, B. Zhang, Y. Sun, H. Lin, Q. Wang, J. Liang, Y. Fan and X. Zhang, *J. Mater. Chem. B*, 2018, DOI: 10.1039/C8TB02999G.

ROYAL SOCIETY OF CHEMISTRY

rsc.li/materials-b

Journal of
Materials Chemistry B

View Article Online
DOI: 10.1039/C8TB02999G

PAPER

Bionic Cartilage Acellular Matrix Microspheres as scaffold for engineering cartilage

Received 00th January 20xx,
Accepted 00th January 20xx

DOI: 10.1039/x0xx00000x

www.rsc.org/

Jun Liu,[a] Xiuyu Wang,[b] Gonggong Lu,[a] James Z. Tang,[c] Yonghui Wang,[b] Boqing Zhang,[a] Yong Sun,[a] Hai Lin,[a] Qiguang Wang,*[a] Jie Liang,[a] Yujiang Fan*[ab] and Xingdong Zhang[a]

Extracellular Matrix (ECM) scaffolds made from decellularized natural cartilage has been successfully used in cartilage lesion repair, but allogeneic cartilage donors are always in shortage and xenogeneic cartilage tissues may have the risk of unknown disease transfer. In this study, we constructed artificial bionic cartilage microspheres by encapsulating MSCs in collagen microspheres and cultured in chondrogenic inducing medium. Then, acellular matrix microsphere (BCAMM) scaffolds were fabricated from cultured microspheres at three different developmental stages. A novel technique was introduced to fabricate BCAMM scaffolds, which achieved in a short time to produce and utilize the scaffolds. Due to the differences in surface morphologies and biological compositions, three BCAMM scaffolds demonstrated different chondrogenic effects. The 10-day BCAMM (10-BCAMM) scaffold showed the best overall results, successfully inducing the MSC chondrogenesis without any additional fetal bovine serum or induction components (TGF-β or dexamethasone). In comparison, the 5-day BCAMM (5-BCAMM) scaffold showed the potential osteogenic effects. The advantage of micron-size BCAMM are outlined, specifically in the easier decellularization process without grinding, homogeneous cell seeding and infiltration, chondrogenic induction and better fitting into the irregular lesion shape.

1. Introduction

Articular cartilage has a very limited self-repair capability due to its low-cell and avascular nature[1,2]. Autologous stem cells were chosen to be the seeding cells due to their potential to differentiate into chondrocytes and more accessible than articular chodrocytes[3]. Current strategies to promote cartilage healing and regeneration have been directed towards improving the chondrogenesis of stem cells by different biomaterials. However, the outcome is not always guaranteed, due to the lack of stem cell's chondrogenic differentiation and the unstable phenotype of induced chondrocyte-like cells[4-6]. Tissue engineering scaffolds are ideally providing cells with biomimetic microenvironments which improve the cell proliferation and functional restoration, or facilitate the differentiation of stem cells.[7] Synthetic scaffolds can be designed to mimic some features of natural Extracellular Matrix (ECM) structure[8-10]. However, these scaffolds couldn't completely reproduce the complicated ECM microenvironments.

ECM scaffolds are another type of scaffolds made from decellularized natural tissues or *in vitro* cultured tissues. They normally offer excellent biological properties to regulate the differentiation of stem cells and have been widely used in clinical treatments, which are associated with skin, cornea, cartilage, tendon and heart valves.[11-16] Allogeneic cartilage donors are always in shortage and xenogeneic cartilage tissues may have the risk of unknown disease transfer.[17-19] Natural mature cartilage are most widely used for the preparation of ECM scaffolds due to its relatively better availability. However, Visser *et al*. observed calcified tissue formation in the cartilage-like tissue when using gelatin methacrylamide hydrogels combined with natural cartilage derived matrix, even with additional chondrogenic factors[14], suggesting that it is difficult to maintain a stable the chondrogenic phenotype of MSC-derived chondrocytes. In the study of Almeida *et al*., scaffolds made from decellularized engineered cartilage loaded with TGF-β1 supported comparable levels of GAG synthesis to native ECM scaffolds.[20]

During the natural cartilage development, mesenchymal stem cells (MSCs) undergo migration, proliferation and condensation.[2,21,22] At different stages, MSCs secrete different proteins, cytokines and growth factors in the ECM, which may result in their different effects in regulating the MSCs differentiation. In our previous study, we found that the

[a] National Engineering Research Center for Biomaterials, Sichuan University, Wangjiang Road 29, Chengdu 610064, China.
*Email: wqgwang@126.com or email: yujiang.fan@163.com

[b] Guangxi Collaborative Innovation Center for Biomedicine, Guangxi Medical University, Nanning, Guangxi 530021, China

[c] School of pharmacy, Faculty of Science and Engineering, University of Wolverhampton, Wolverhampton, WV1 1LY, United Kingdom

Electronic Supplementary Information (ESI) available: Additional figures. See DOI: 10.1039/x0xx00000x

chondrogenesis of MSCs in three-dimensional (3D) collagen hydrogel microsphere (CHM) culture system could partly mimic the natural process of cartilage formation, especially for the cell migration, condensation, abundant cartilage specific matrix secretion and low hypertrophic gene expression.[23] The cartilage-like tissue formed from above culture were named bionic cartilage microspheres (BCM), which contained the homogeneous cartilage specific matrix, including glycosaminoglycans (GAGs) and type II collagen.

In this study, we developed a novel method to obtain acellular matrix from BCM cultured for different time to mimic the MSCs chondrogenic differentiation at different stages (Scheme 1). We demonstrated the advantages of bionic cartilage acellular matrix microspheres (BCAMM) during its fabrication and ultlization: (1) 500 mg BCM (corresponding volume was ~ 1000 mm^3) could be fabricated from 3.6 $\times 10^6$ cryopreserved MSCs (passage 2) within 15 days; (2) Micron size of the BCM would allow a new decellularization methodology to obtain BCAMM without grinding to preserve the natural ECM structure; (3) Large surface area and micron-size scale of the BCAMM would further enhance the cell adhesion, cell infiltration, mass transfer and better integration into the irregular lesion area; (4) Extremely low number of MSCs (only 1 ~ 4 $\times 10^4$ cells/mg) were required to seed on the scaffold, which reduced the requirement of patient's MSCs in clinical and the *in vitro* cell expansion duration and cost. The obtained BCAMM expressed different chondrogenic effects due to the differences in surface morphologies and biological compositions. The decellularization effectiveness, key ECM reservation and the chondrogenic effects of BCAMM at different developmental stages were investigated.

2. Materials and Methods

Materials

Collagen type I was extracted from a new born calf skin and dissolved in a 0.5M acetic acid solution. Alpha-modified Eagle's Medium (α-MEM) and Dulbecco's Modified Eagle Medium (DMEM) were purchased from Hyclone. 4'-6-diamidino-2-phenylindole (DAPI) was obtained from Beyotime Biotechnology, China. DNAse I, L-ascorbic acid 2-phosphate, L-proline, Dexamethasone, ITS+Premix was purchased from Sigma-Aldrich, USA. Nonessential amino acid (NEAA) and Fetal Bovine Serum (FBS) were obtained from Gibco, USA. TGF-β1 was obtained from PeproTech, USA. Fluorescein diacetate (FDA), propidium iodide (PI), Triton X-100 and alizarin red were obtained from Solarbio, China. TRITC-labeled phalloidin was purchased from YEASEN Bio, China. Anti-TGF-β1 antibody (ab190503) and anti-BMP2 (ab6285) were purchased from Abcam, USA. Anti-IGF1 (nbp2-34361), anti-VEGF (nbp2-45235), anti-PEDF (mab1177), anti-COL1 (nb600-450), anti-COL2 (nbp2-33343) antibodies were obtained from NOVUS, USA. Alexa Fluor488-affiniPure Goat Anti-Mouse IgG was purchased from Jackson ImmunoResearch, USA. Goat serum and polyperoxidase-anti mouse IgG were obtained from ZSGB-BIO, China. Blyscan GAG assay kit was obtained from Biocolor, UK. All other chemicals were purchased from Chengdu Kelong unless otherwise specified.

MSCs isolation

In brief, neonatal New Zealand white rabbit (Breeding Farm for Sichuan Provincial Experimental Animal Special Committee) was sacrificed. Under sterile condition, long bones were collected and the bone marrow was flushed out with α-MEM containing 20% FBS and antibiotics (penicillin 100 U/mL, streptomycin 100 μg/mL) by a syringe. Bone fragments were removed by cell strainer (70 μm, BD Falcon, USA). After centrifugation, filtered bone marrow cells were resuspended in the medium and cultured in the 10-cm cell culture dishes at 37°C with a humidified atmosphere of 5% CO2. Non-adherent cells were removed by replacing fresh medium after a 24 h

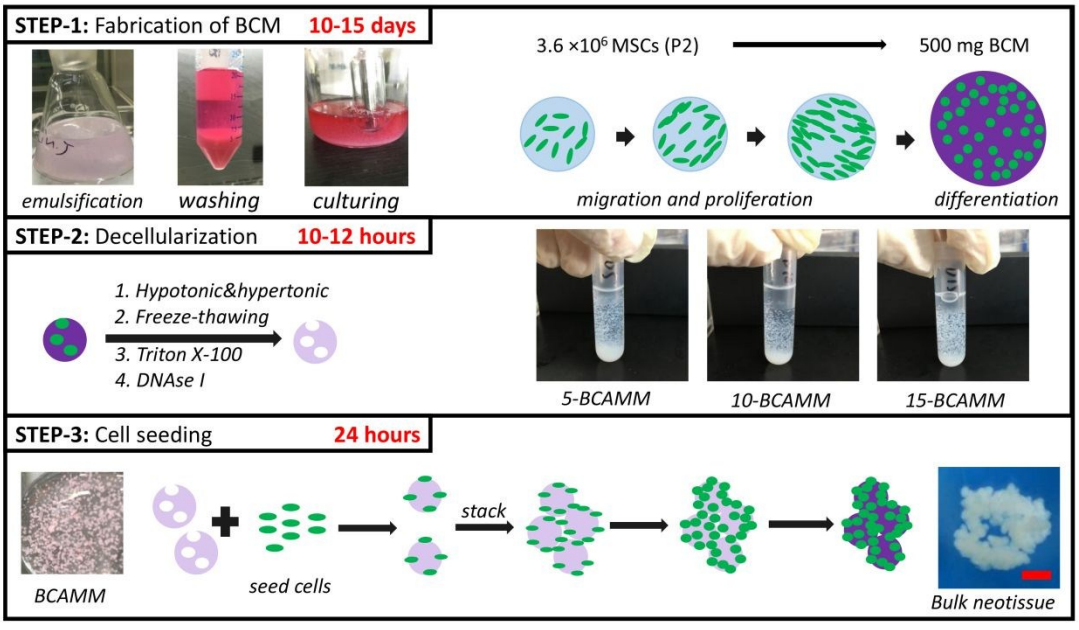

Scheme 1. Schematic representation of BCAMM fabrication process. Scale bars represented 1 mm

culture. The MSCs were passaged until a confluence of 90%. The MSCs of forth passage were used to fabricate CHM.

Fabrication of bionic cartilage microsphere (BCM)

Collagen solution was neutralised with 1M NaOH. MSCs were counted and resuspended in the culture medium. Collagen solution was adjusted to the final concentration of 6 mg/mL with the cell solution. The final cell density was 5.0×10^6 cells/mL. The collagen-cell mixture was injected into the stirring PDMS and the speed was set at 500 rpm. The system was moved to a 37°C water bath after 10 min stirring and kept stirring for another 20 min. After gelation, CHM were collected and washed with the culture medium 3 times. CHM were then cultured in a MSCs medium for 6 hours and then replaced the medium with a chondrogenic medium (DMEM medium, 1% penicillin-streptomycin, 90 mg/mL L-ascorbic acid 2-phosphate, 0.35 mM L-proline, 100 nM dexamethasone, 10 ng/mL TGF-β1, 1% insulin-transferrin-selenite-linoleic acid (ITS+) and 1% NEAA) to induce cartilage-like tissue regeneration. The culture was conducted *in vitro* for a total of 15 days, and the BCMs at day 5, 10, and 15 were collected respectively.

Fabrication of bionic cartilage acellular matrix microsphere (BCAMM):

BCMs harvested at different time points (5 days (5-BCM), 10 days (10-BCM), and 15 days (15-BCM)) were decellularized to fabricate the corresponding BCAMMs. Firstly, BCMs were washed with a hypotonic solution and a hypertonic solution 3 times. The BCMs were frozen in liquid nitrogen and thawed in a 37°C water bath 6 times. Then BCMs were immersed in the 0.5% Triton X-100 solution containing 20mM ammonium hydroxide for 20 min and washed with water 3 times. 20KU DNAse I was dissolved in 1 mL Tris-HCl buffer (25 mM, Ph=7.5) containing 50% glycerol, 5 mM $CaCl_2$ and 5 mM $MgCl_2$ as stock solution. Before using, the DNAse I stock solution were diluted 100-fold with reaction solution (Ph=7.5) which contains 10 mM Tris-HCl and 2 mM $MgCl_2$ to the prepare the working solution. The 200U/mL DNAse I working solution was used to remove the DNA in the BCM at 37°C for 3 hours and the solution was replaced twice every 3 hours. Finally, BCMs were washed with Triton X-100 solution and water 3 times, followed by crosslinked with 0.1% glutaraldehyde for 20 min. BCAMMs were frozen by liquid nitrogen and stored in the refrigerator at -20°C before use.

Removal of DNA

BCAMMs fabricated from different BCMs (5-BCAMM, 10-BCAMM and 15-BCAMM) were fixed with 4% paraformaldehyde and then embedded in paraffin. The 6 μm sections were prepared and stained by DAPI to confirm the removal of cells.

Surface morphology

Environmental scanning electron microscope (ESEM, FEI Quanta 650) was used to character surface morphologies of scaffolds.

Cytokines in the scaffold

Immunohistochemical staining was used to detect remnant cytokines in scaffolds. After blocked with goat serum for 2 hours, sections were incubated with primary antibodies of TGF-β1, BMP-2, IGF-1, PEDF and VEGF for 10 hours. Then the sections were washed with TBS 3 times, followed by incubating with second antibody in the cassette. The sections stained by the same antibody were imaged by confocal laser scanning microscopy (CLSM, TCS SP 5, Leica) with the same parameters.

Cell seeding and culture

MSCs of third passage were seeded on the BCAMM at the density of 4×10^4 cells/mg and cultured in the MSCs culture medium (α-MEM containing 10% fetal bovine serum) for adhesion. To eliminate the effect of cytokines in the serum and the differentiation effect of dexamethasone (which was confirmed in the pre-experiment, in the **Figure S1**), we used the culture medium without TGF-β, dexamethasone and serum. After a 24 hours cells adhesion, samples were cultured in the DMEM medium containing 1% penicillin-streptomycin, 90 μg/mL L-ascorbic acid 2-phosphate, 0.35 mM L-proline, 1% ITS+Premix and 1% nonessential amino acid for 28 days.

Cell viability and cell morphology

Cell viability was assessed with FDA/PI double staining after 1 and 7 days culture. All samples were washed with PBS and incubated in the FDA-PI (1 μg/mL) dyeing solution for 5 min. Then samples were washed with PBS again before observed with CLSM. The CLSM pictures were analysed by ImageJ software (1.51j8, National Institutes of Health) to calculate cells' circularity. For cell morphology, samples were stained with TRITC-labeled phalloidin for 20 min and DAPI for 30 seconds to show the cytoskeleton, followed by washed with PBS before observed with CLSM.

Gross morphology and weight change of samples

Samples at day 7, 14 and 28 were imaged by digital camera and the size was measured. To observe degradation and neo-tissue formation, the wet weight and dry weight of samples were measured by an electronic analytical balance (Mettler Toledo XP205).

Immunohistochemical staining

Immunohistochemical staining was used to confirm the secretion of collagen type I and II in the matrix. After *in vitro* culture, samples were washed with PBS and then fixed with 4% paraformaldehyde at 4°C for 24 h, followed by paraffin section in 6 μm. For immunohistochemical staining, primary antibodies of COL1 and COL2 were used. Sections were blocked with a goat serum for 2 hours and then incubated with primary antibodies at 4°C for 10 hours. After being washed with TBS 3 times, sections were immersed in the 0.3% H_2O_2 for 10 min, followed by polymer helper for 20 min and second

View Article Online
DOI: 10.1039/C8TB02899C

antibody for 20 min. Finally, Diaminobenzidine (DAB) was used to visualise the peroxidise labelled antibody for 5 min and observed under microscope.

Alizarin Red staining of mineral deposition

Alizarin Red was used to detect the mineral deposition in the BCAMMs after *in vitro* culture. Sections were immersed in the 95% ethanol before 5 min staining of Alizarin Red S (pH=4.2). After washing with water to remove residual staining liquid and dehydration, slides were observed under microscope.

GAG staining and quantitation

To characterise the remnant GAGs in the BCM before or after decellularization and the GAGs secretion by MSCs in the BCAMM, the lyophilised samples were digested in the papain solution (0.1mg/mL) at 60℃ for 12 hours before measured with the Blyscan™ GAG assay Kit. Briefly, a 40 μl supernatant was mixed with Blyscan™ dye reagent. After centrifugation, the sGAG-dye complex was dissolved in the dissociation reagent and followed by the measurement of absorbance at 650 nm in the reader. Histological staining was used to confirm the secretion and distribution of cartilage specific matrix in samples. For histological staining, Toluidine Blue (TB) was used to detect GAGs by the positive staining with a purple colour.

DNA content

DNA contents in the BCM before or after decellularization were determined to confirm the removal of cell nucleus. The proliferation of MSCs on the BCAMM was also measured by the same method. Briefly, a 10 μL digestion liquid was added into 2mL of a Hoechst 33258 solution and measured by fluorometry.

Micro-CT

To detect the calcific tissue, samples underwent micro-CT scans (VivaCT80, SCANCO Medical). The parameters were 70 kV tube voltage, 114 mA tube current and 50 μm resolution. Images were reconstructed by Mimics 17.0 software (Materialize). The degree of calcification was presented as the ratio of calcific tissue volume to total tissue volume.

Statistical Analysis

All results were presented as mean ± standard error of the mean (SEM). The one-way ANOVA was carried out to test the significance of the differences among the study groups. Statistical differences were shown with three significance levels; *P<0.05, **P <0.01 and ***P < 0.001.

3. Results

3.1. Fabrication of BCAMM scaffolds

3.1.1. Effective decellularization of BCM

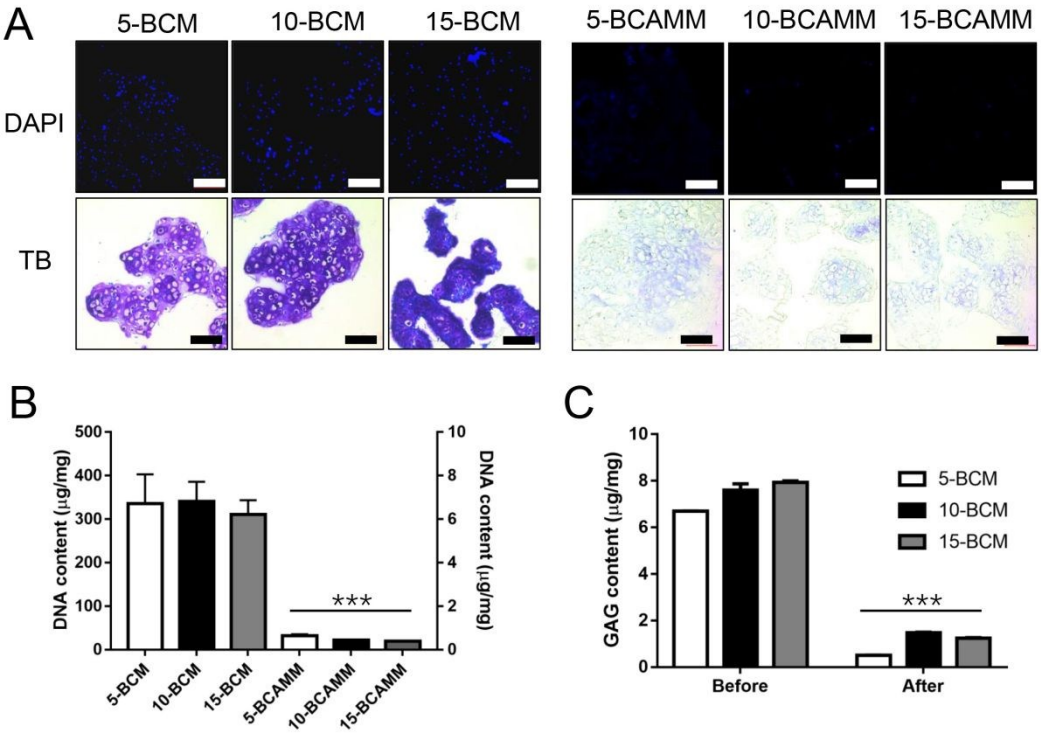

Figure 1. Decellularization effect. A) DAPI and TB staining of 5-BCM, 10-BCM, 15-BCM and 5-BCAMM, 10-BCAMM, 15-BCAMM. Scale bars represented 100 μm. B) DNA content of BCMs (Left y-axis) and BCAMMs (Right y-axis). C) GAG content of BCMs before and after decellularization. Data are expressed as the mean ± SEM (n=3~4). ***presents P<0.001.

The effects of the decellularization process on the BCM were shown in **Figure 1**. After DNAse I treatment, DNA in the BCM was degraded by enzymes. The two rows of Figure 1A show DAPI staining of DNA before (BCM) or after (BCAMM) decellularization. The DNA content of BCM and BCAMM was quantified and shown in the Figure 1B. After decellularization, only about 0.11% ~ 0.19% DNA was left in the BCAMM, which indicating that DNA was effectively washed away by this decellularization method, in agreement with the findings of DNA staining in Figure 1A. The second row of Figure 1A showed the TB staining of BCM or BCAMM. Before decellularization, GAGs were intensively stained in the BCM. After treatment with decellularization regents, most of GAGs were washed off, leaving an almost invisible ECM network. The GAG content analysis before (BCM) or after (BCAMM) decellularization in Figure 1C supports this with 6.4%, 19.7% and 18.4% of GAGs remaining in the 5-BCAMM, 10-BCAMM and 15-BCAMM after the decellularization.

3.1.2. Distinct surface morphology of different BCAMMs

Surface morphologies of BCMs and BCAMMs in **Figure 2** revealed some interesting features which were in favour of cell attachment, proliferation, and possibly differentiation. All BCM surfaces showed distinct cellular-like structures with entities less than 10 μm. In comparison, All BCAMM surfaces lost the cellular-like structures. The 5-BCAMM and 10-BCAMM demonstrated a distinct featured morphology with a rougher surface compared to that of the 15 BCAMM, which had shown the smoothest surface among the three.

3.1.3. Key cytokines remained in BCAMMs

The immunohistochemical staining of TGF-β1, BMP-2, IGF-1, PEDF and VEGF were revealed in **Figure 3**. Among three BCAMMS, the BMP-2, IGF-1 and VEGF staining intensities increased in BCAMMs. In contrast, PEDF staining was observed in 5-BCAMM and 10-BCAMM, but the intensity was decreased in the 15-BCAMM. Moreover, the TGF-β1 staining wasn't visually different in 5-BCAMM, 10-BCAMM and 15-BCAMM samples.

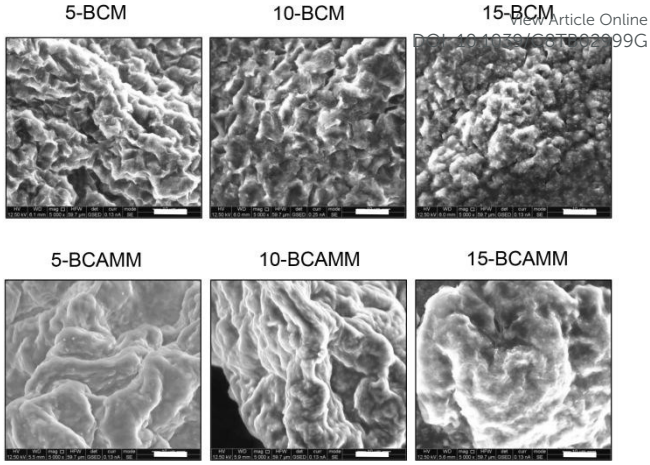

Figure 2. ESEM image of surface morphologies of 5-BCM, 10-BCM, 15-BCM and 5-BCAMM, 10-BCAMM, 15-BCAMM. Scale bars represented 10 μm.

3.2. MSCs culture on BCAMMs

3.2.1. BCAMMs impact on cell morphology and proliferation

Different effects of BCAMMs on the seeding cells' morphology and proliferation were shown in **Figure 4**. It was clear that most of cells were viable (green) after 7 days' culture without visible death of cells (Figure 4A). In comparison, there were visually more cells and cell interconnection on the 5-BCAMM and 10-BCAMM than the 15-BCAMM at day 1. As MSCs were initially seeded at the same cell density in all samples, it also reflected to the cell seeding efficiency of the 5-BCAMM and 10-BCAMM in consideration of the day-1 FDA-PI staining. The cell morphology was studied by exploitation of the F-actin staining (Figure 4B) and validated with circularities of cells using ImageJ software (Figure 4C). The combination of phalloidin & DAPI staining showed the cell skeleton (red) and nucleus (blue). The day 1 results indicated that most MSCs on the 5-BCAMM had fibroblast-like morphology and most MSCs on the 15-BCAMM had spherical morphology; while those on the 10-BCAMM did not have such preferences. To validate these observations, the roundness of MSCs was further analysed by calculating the circularities of cells. The average

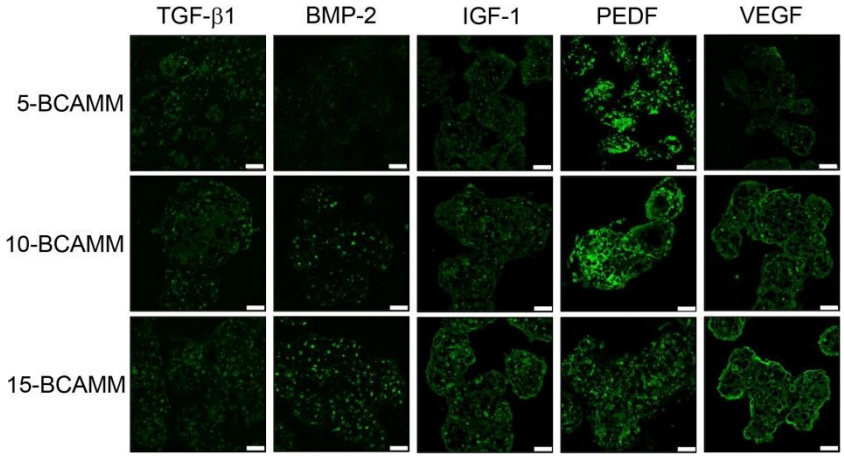

Figure 3. Immunohistochemical staining of TGF-β1, BMP-2, IGF-1, PEDF and VEGF in the BCAMMs. Scale bars represented 50 μm.

View Article Online
DOI: 10.1039/C8TB02999G

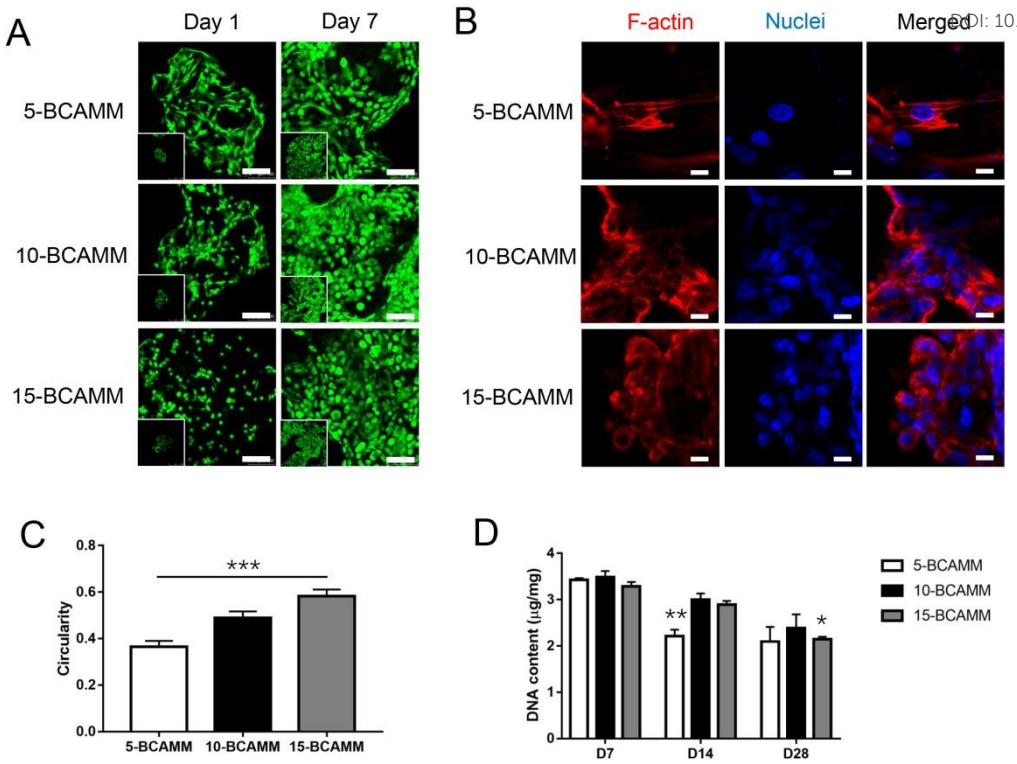

Figure 4. MSCs culture on BCAMM. A) FDA/PI image of MSCs on day 1 and day 7. Scale bars represented 100 μm. B) F-actin staining image on day 1. Scale bars represented 10 μm. C) Circularity of MSCs on the day 1. D) DNA content of total cells on the BCAMM. Data are expressed as the mean ± SEM (n=3). * presents P<0.05, ** presents P<0.01, ***presents P<0.001.

circularities of MSCs on the 5-BCAMM, 10-BCAMM and 15-BCAMM at day 1 were 0.366, 0.490 and 0.582, respectively. The higher value means the more roundness of cells, indicating that cells were more spherical in the sample. On day 7, the cell morphology wasn't visually changed much, as some fibroblast-like cells were still on the 5-BCAMM. Compare to day 1, there were visually much more cells at day 7 on all samples, suggesting that all three BCAMMs had a good cytocompatibility and could support cells' proliferation without additional serum. The dark area without green fluorescence was observed in the 5-BCAMM at day 7, which was possibly caused by the loss of support to the cell adhesion after the scaffold degradation. After the initial increase in cell number, the DNA content decreased gradually from day 7 to day 28 (Figure 4D), which reflected the decrease of the cell number. According to the 6.5~9.3 pg DNA per MSCs reported by literature,[24-26] the initial theoretical maximum DNA content was 0.74 μg/mg and that confirmed the MSCs proliferation during the period of day 1 to day 7. Those phenomena might be caused by the chondrogenic differentiation of MSCs, as the DNA content had been previously reported to decline during chondrogenesis. [27-29]

3.2.2. Influence of BCAMMs on GAGs synthesis

After seeding cells, the appearance and the solid content of BCAMMs changed. On the day 7, the initial micron size BCAMMs (showed in the Scheme 1) had cohered to be one larger bulk (**Figure 5**A). All BCAMM showed great integration ability. The Figure 5B showed the TB staining of GAG secreted by the MSCs in various BCAMM samples at different time points. Among three samples, sample 10-BCAMM had a visually more positive staining increase with time. 5-BCAMM registered positive staining peaks at Day 14 but faded from Day 14 to Day 28. Fastest degradation speed of 5-BCAMM scaffold resulted in shrinkage and even breakdown of the matrix network in comparison to those of the sample 10-BCAMM that demonstrated a significant different matrix network corresponding to the positive staining. Due to the slowest degradation speed of scaffold, sample 15-BCAMM had slower inner cell growth and secretion of cartilage specific matrix. Furthermore, the quantitated GAG content in all three samples on day 28 also echoed the histological TB staining result (Figure 5C), and the GAGs synthesised in sample 10-BCAMM had achieved significantly more quantity than the 5-BCAMM and 15-BCAMM samples. Solid contents of three samples on day 0, 7, 14 and 28 were calculated and showed in the Figure 5D. The solid content of the 5-BCAMM decreased before the day 7 and then increased steadily up to day 28, whereas that of the 10-BCAMM' had no change in the first 7 days before the steady weight increase with time up to day 28. In comparison, the solid content of sample 15-BCAMM increased with time but at a lower rate except the first 7 days. Among all three samples, 10-BCAMM had achieved the highest solid content (33.26%) on day 28, followed by 5-BCAMM (29.30%), and 15-BCAMM (27.88%).

View Article Online
DOI: 10.1039/C8TB02999G

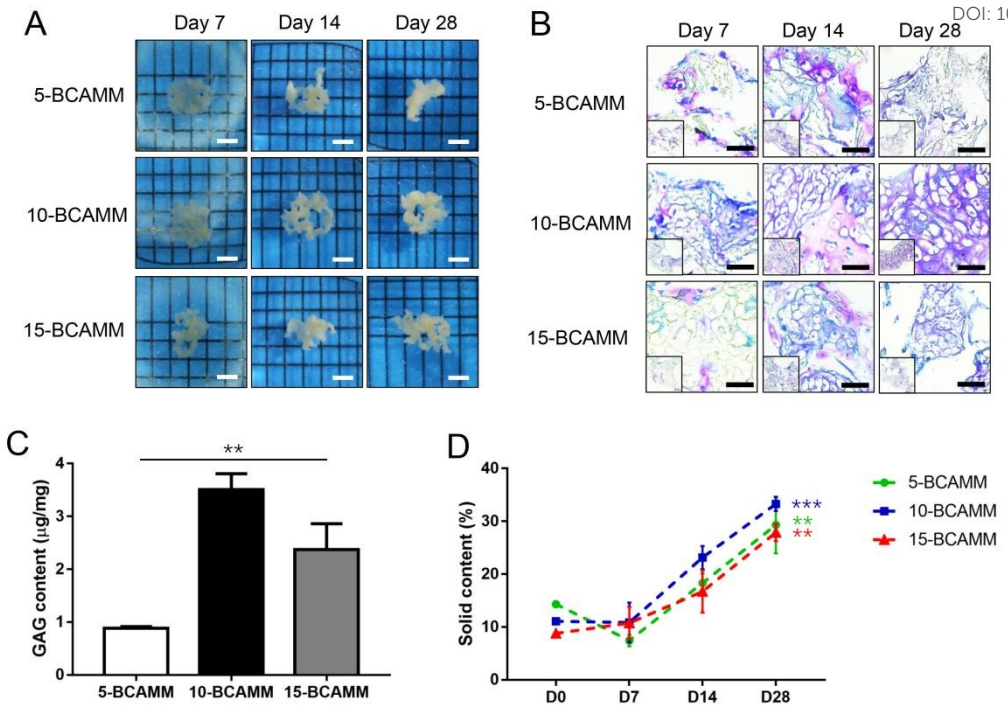

Figure 5. A) Metallographic microscope pictures of samples. Scale bars represented 1000 μm B) TB staining image of BCAMMs after culture with MSCs. Scale bars represented 50 μm. C) GAG content of BCAMMs after culture with MSCs. D) Solid content of BCAMMs after culture with MSCs. Data are expressed as the mean ± SEM (n=3). ** presents P<0.01, ***presents P<0.001.

3.2.3. Collagen deposition

Figure 6 shows the immunohistochemical staining of collagen type I and collagen type II, which reflect the accumulation of cartilage specific collagen. Throughout the 28 day's culture, sample 5-BCAMM showed the highest collagen type I staining among three samples, and its staining intensity increased with time in Figure 6A. There was less collagen type I staining in sample 10-BCAMM at day 7 and the staining kept at a low level at both day 14 and 28 days. In contrast, sample 15-BCAMM had minimal collagen type I staining at day 7 and 14, but the staining increased a little at day 28. Collagen type II was the specific collagen of articular hyaline cartilage. The day 1 staining (Figure 6B) showed the collagen type II preserved from the BCMs. As the 15-BCAMM scaffold was fabricated from a more matured BCM, the collagen type II staining was more intensive than other two BCAMMs. After 28 days, the collagen type II staining intensity was increased in all three scaffolds, despite the 5-BCAMM structure collapsed.

3.2.4. The 5-BCAMM culture leads to Mineral deposition

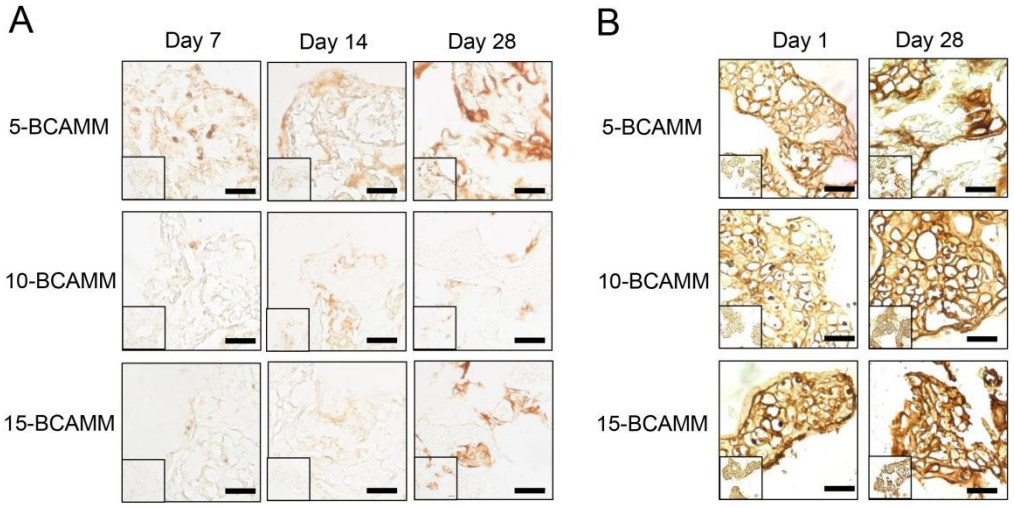

Figure 6. Immunohistochemistry of BCAMMs after culture with MSCs. A) Collagen Type I. B) Collagen Type II. Scale bars represented 50 μm.

View Article Online
DOI: 10.1039/C8TB02999G

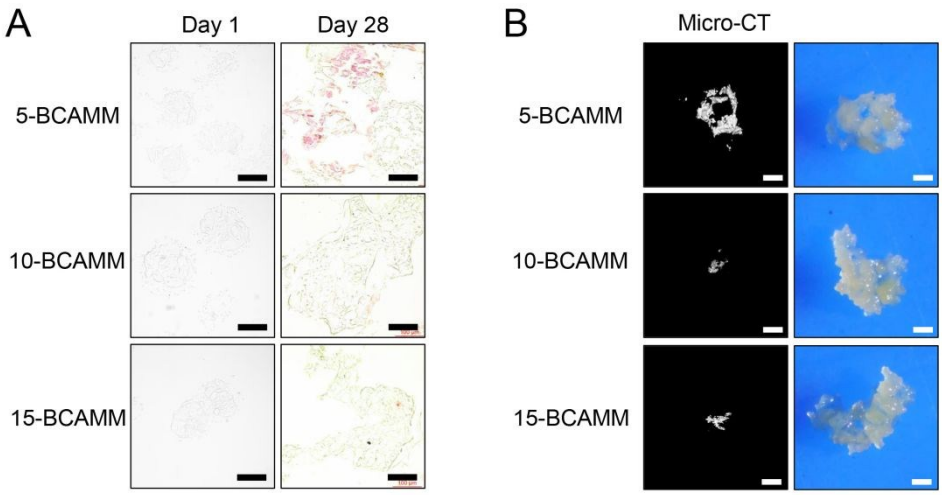

Figure 7. Mineralization deposition in the BCAMMs after culture with MSCs. A) Alizarin Red staining. Scale bars represented 100 μm. B) Micro-CT image of calcified tissue in samples. Scale bars represented 500 μm.

Different degrees of mineral deposition could be found in the BCAMMs after cultured with MSCs (**Figure 7**). All samples had no mineralization deposition at day 1 as revealed by the alizarin red staining (Figure 7A). On day 28, there were lots of positive red staining areas in sample 5-BCAMM, indicating the mineralization deposition. In comparison, there were less to none staining areas to be observed in sample 15-BCAMM and 10-BCAMM. Micro-CT images (Figure 7B) showed the size of the calcific tissue in the whole sample, and the result was consistent with the alizarin red staining. Sample 5-BCAMM had the largest calcific volume, which occupied about 28.4% of total sample volume. In contrast, the calcific volumes of sample 10-BCAMM and 15-BCAMM were much smaller and the percentages were about 2.8% and 3.1%, respectively. Similar results were also observed in another experiment under the culture medium containing 1% serum that sample 5-BCAMM and sample 15-BCAMM had calcific tissue while none mineralization was found in the sample 10-BCAMM (**Figure S2**).

4. Discussion

Based on our previous study, bionic cartilage microspheres could be made *in vitro* within 15 days and the chondrogenic genes expression was stable.[23] Combining the collagen microspheres culture system and the microsphere decellularization technique, we had managed to fabricate three ECM scaffolds (5-BCAMM, 10-BCAMM, and 15-BCAMM) from allogeneic MSCs, and conducted a comprehensive evaluation to their chondrogenic inductivities. To avoid any potential chondrogenic effect from cell culture medium and to mimic the limited nutrient microenvironment in the natural articular cartilage, we used the basic culture medium without any FBS that may contain extra nutrients and various unknown cytokines. Neither TGF-β nor dexamethasone was added in order to avoid their induction ability, as observed in our pre-experiments (in Supplementary Information Figure S1). To our knowledge, this is the first study that successfully induced the *in vitro* chondrogenic differentiation of MSCs solely by the 3D decellularized scaffold, without any additional serum and induction components.

Seeding cells' fate would be greatly affected by the properties of scaffolds, including the cytotoxicity, chemical contents, surface morphology and degradation speed. [8,30-33] In our study, it was found that differences in three BCAMMs clearly influenced the cell seeding efficiency and the cell morphology. FDA-PI images demonstrated that more cells were attached on sample 5-BCAMM and 10-BCAMM than 15-BCAMM scaffolds on day 1, and the Phalloidin & DAPI staining showed a high percentage of fibroblast-like cells in the sample 5-BCAMMs but more circular cells were observed in sample 15-BCAMMs. The phenomenon was coincided with the study of Hallab *et al*. that polymers showed an increase of the cellular adhesion strength associated with the increase of the surface roughness.[34] According to previous study, collagen Type I in the microspheres decreased with the extended culture of BCM. Thus the 5-BCM might remain more collagen type I due to the shorter culture time, and the more remnant collagen type I in 5-BCAMM might also facilitate the adhesion of cells. In addition, it is generally believed that fibroblast-like cells would proliferate faster than circular cells and apply more contraction force to the surrounding scaffold network.[33] However, with the highest percentage of fibroblast-like cells in sample 5-BCAMM, its fast degradation (TB staining at day 7) resulted in a lower cell number at latter stages (14 and 28 days). In contrast, more circular cells in sample 15-BCAMMs resulted in a lowest seeding efficiency and proliferation rate in all three scaffolds, but its degradation was the slowest throughout the culture period. Sample 10-BCAMMs had a balanced number of both fibroblast-like cells and circular cells, which resulted in the highest DNA content at day 28.

It had been widely accepted that a high cell density would in favour of chondrogenic differentiation,[35-37] but the result of sample 5-BCAMMs showed that the fast degradation of scaffold before neo-tissue formation caused by too much

View Article Online
DOI: 10.1039/C8TB02999G

spread cells was not a good condition. In contrast, the best overall results achieved by the 10-BCAMM had perfectly proved the tissue engineering theory that the degradation speed should match speed of the neo-tissue formation.[38-40] Furthermore, it had been reported that the spheroid phenotype of MSCs would help to promote the chondrogenesis and the fibroblast-like phenotype would contribute to the osteogenesis. In the study of Kang et la., spreading MSCs on the graphene oxide-collagen scaffold had a higher expression of ALP and OP.[41] Another study of Cao *et al.* also showed that the spreading chondrocytes had a lower expression of COL2, AGG and SOX9. [42] In coincide with above literatures, our results demonstrated that sample 5-BCAMM with more fibroblast-like cells had finally turned into a large amount of calcified tissue, while sample 10-BCAMM and 15-BCAMM with more circular cells had resulted in more cartilaginous tissue.

Soluble GAGs in the ECM would be easily washed off during the decellularization procedure, as Falguni *et al*. found that only 25% of GAGs were remained after decellularization of natural cartilage.[31] In our study, we also couldn't help to prevent this common phenomenon. However, our scaffolds had managed to preserve many key ECM components after decellularization. Various cytokines remained in the different BCAMMs might be the vital factor leading to the different inducibilities of three BCAMM scaffolds. Many studies had reported that BMP-2 was an important cytokine during chondrogenesis, with the function to enhance the effects of TGF-β and promotes maturation of chondrocytes.[43-45] As another important cytokine, IGF-1 was found to be responsible for promoting accumulation of cartilage matrix. [21,43,46,47] There were more IGF-1 remained in sample 10-BCAMM and 15-BCAMM than 5-BCAMM; suggesting the former two scaffolds may theoretically hold a higher chondrogenic inducibility than sample 5-BCAMM. It explained well that sample 10-BCAMM and 15-BCAMM had resulted in more GAG and type II collagen production than sample 5-BCAMM. In the study of Rong *et al*., MSCs were seeded on PLGA mesh and fabricated ECM scaffolds after 7 or 21 days culture.[22] The results showed that 7-day-ECM sample was richer in the cartilage matrix than 21-day-ECM, which was consistent with our result that sample 10-BCAMM was better than sample 15-BCAMM. Together, it encouraged the investigations of ECM scaffolds during the developmental stage.

Tissue mineralization was a common phenomenon during chondrogenesis of MSCs *in vitro* and cartilage regeneration *in vivo*. Farrell *et al.* found that MSCs-seeded agarose hydrogels without TGF-β were heavily calcified after a long time culture.[6] A high degree of calcification was found in gelatin methacrylamide hydrogels with embedded MSCs and cartilage-derived matrix particles after subcutaneous implantation.[14] VEFG had a great effect on the neovascularization during endochondral bone formation and PEDF could inhibit angiogenesis and counteract with VEGF.[43,48,49] Sample 5-BCAMM contained the most PEDF and the least VEGF. However, the failure of chondrogenesis and fibroblast-like morphology of MSCs led to osteogenesis of sample 5-BCAMM with the heaviest calcification, as evidenced by the collagen type I and alizarin red staining. There was a slight difference between sample 10-BCAMM and 15-BCAMM that more calcific tissue was quantified in sample 15-BCAMM probably because of the higher VEGF content in the 15-BCAMM that could enhance the collagen type I secretion and decrease the GAG secretion of MSCs during the late period.[50,51]

ECM scaffolds had been used in clinical treatments for decades. However, due to the shortage of allogenic tissue and the unknown disease risk of xenogeneic tissues, harvesting the sufficient number of suitable ECM scaffolds in clinical had been always a challenge. Advantage of microsphere culture system had been reported previously in our research, as more GAG production and more stable phenotype was achieved by the chondrocyte cultured in microspheres compare to bulk hydrogel.[52,53] In this study, we had demonstrated a cost-effective methodology to fabricate ECM scaffolds (BCAMM) by combining the collagen microspheres culture system and the microsphere decellularization technique. Based on our previous study, about 500 mg BCM (= 1000 mm^3 volume) could be fabricated from 3.6×10^6 cryopreserved MSCs (P2) within 7~17 days from time point of recovering cells. To minimise DNA residues in the ECM scaffold, tissues were normally cut into pieces and grinded into slurry before decellularization, especially for dense tissues like cartilage. However, grinding tissues into slurry during the decellularization process would partly destroy the tissue structure and consequently undermine the ECM microenvironments, which was crucially important for MSCs differentiation.[30,54] Unlike the traditional ECM scaffold, micron-sized BCMs could be decellularized to BCAMMs without grinding. Compare to the previous decellularization technique for chondrocytes microspheres[55], our decellularization process effectively removed 99.89% DNA without using sodium deoxycholate, which was an anionic, bile-acid detergent that might disrupt and dissociate many types of protein interactions. Consequently, the gentler decellularization process preserved the crucial microstructure and various cytokines at different developmental stages to influence the chondrogenic differentiation of MSCs. Among BCAMM scaffolds prepared at different time points, the 10-BCAMM showed the best chondrogenic induction ability and a better anti-mineralisation ability. Furthermore, as the MSC percentage gradually declined with age in adult,[56,57] we tested an even lower cell seeding density of 1×10^4 cells/mg on the BCAMMs, by conducting the *in vitro* culture in the culture medium with 1% FBS. After 28 days, a large mass of GAGs was secreted as shown in the Figure S2, which had demonstrated the usefulness of BCAMMs with very low cell numbers. It would be a welcomed advantage to use less MSCs in clinical; in terms of the treatment complexity, patient's welfare and the cost.

5. Conclusion

BCAMM scaffolds derived from MSCs at different differentiation stages had all demonstrated chondrogenic effects to MSCs without any additional serum or induction components. The best chondrogenic effects were achieved by sample 10-BCAMM, which not only had the highest cartilage

matrix production, but also inhibited the matrix calcification. The study also provided a novel technique to fabricate micron-size BCAMM scaffolds using the artificial ECM source of BCM. The BCM could be effectively decellularized with preservation of its natural ECM structures, consequently providing a large surface area for cell adhesion and proliferation. The fabrication of the BCAMM may offer a viable source with potential advantages to replace the allogenic cartilage ECM in clinic applications.

Acknowledgement

This work was supported by the National Key Research Program of China (2016YFB0700804 and 2016YFC1103202), the National Key Technology R&D Program of China (2012BAI42G01), the Natural Science Foundation of China (31130021 and 51403134), the Fundamental Research Funds for the Central Universities (YJ201747), the Sichuan Science and Technology Program (2018RZ0039), Guangxi Collaborative Innovation Center of Biomedicine (GCICB-IE-2017008) and the 111 Project (No. B16033).

Notes

The authors declare no competing financial interest.

Abbreviations

ECM, extracellular matrix; MSCs, mesenchymal stem cells; BCM, bionic cartilage microsphere; BCAMM, bionic cartilage acellular matrix microsphere; 3D, three-dimensional; CHM, collagen hydrogel microsphere; GAG, glycosaminoglycans; ITS+, insulin-transferrin-selenite + linoleic acid; NEAA, nonessential amino acid; VEGF, vascular endothelial growth factor; PEDF, pigment epithelium-derived factor; DAB, diaminobenzidine; TB, Toluidine Blue.

References

1 J. Buckwalter and H. Mankin, Arthritis Rheum, 1998, 41, 1331–42.
2 S. Camarero-Espinosa, B. Rothen-Rutishauser, E. J. Foster and C. Weder, Biomater. Sci., 2016, 4, 734–767.
3 L. Yan, J. M. Oliveira, A. L. Oliveira and R. L. Reis, ACS Biomater. Sci. Eng., 2015, 150220124046001.
4 K. M. Hubka, R. L. Dahlin, V. V Meretoja, K. Kasper and A. G. Mikos, Tissue Eng. Part B, 2014, 20, 1–50.
5 V. V. Meretoja, R. L. Dahlin, S. Wright, F. K. Kasper and A. G. Mikos, Biomaterials, 2013, 34, 4266–4273.
6 M. J. Farrell, M. B. Fisher, A. H. Huang, J. I. Shin, K. M. Farrell and R. L. Mauck, J. Biomech., 2014, 47, 2173–2182.
7 N. Annabi, A. Tamayol, J. A. Uquillas, M. Akbari, L. E. Bertassoni, C. Cha, G. Camci-Unal, M. R. Dokmeci, N. A. Peppas and A. Khademhosseini, Adv. Mater., 2014, 26, 85–124.
8 S. Bian, M. He, J. Sui, H. Cai, Y. Sun, J. Liang, Y. Fan and X. Zhang, Colloids Surfaces B Biointerfaces, 2016, 140, 392–402.
9 K. Ren, C. He, C. Xiao, G. Li and X. Chen, Biomaterials, 2015, 51, 238–249.
10 L. Wang and J. P. Stegemann, Biomaterials, 2010, 31, 3976–3985.
11 B. Nyambat, C. Chen and P. Wong, J. Mater. Chem. B, 2018, 979–990.
12 Y. Hashimoto, S. Funamoto, S. Sasaki, T. Honda, S. Hattori, K. Nam, T. Kimura, M. Mochizuki, T. Fujisato, H. Kobayashi and A. Kishida, Biomaterials, 2010, 31, 3941–3948.
13 L. Utomo, M. M. Pleumeekers, L. Nimeskern, S. Nürnberger, K. S. Stok, F. Hildner and G. J. V. M. van Osch, Biomed. Mater., 2015, 10, 015010.
14 J. Visser, D. Gawlitta, K. E. M. Benders, S. M. H. Toma, B. Pouran, P. R. van Weeren, W. J. A. Dhert and J. Malda, Biomaterials, 2015, 37, 174–182.
15 J. S. Cartmell and M. G. Dunn, J. Biomed. Mater. Res., 2000, 49, 134–140.
16 S. Cebotari, I. Tudorache, T. Jaekel, A. Hilfiker, S. Dorfman, W. Ternes, A. Haverich and A. Lichtenberg, Artif. Organs, 2010, 34, 206–210.
17 J. A. B. Cindy Chung, Adv. Drug Deliv. Rev., 2008, 60, 243–262.
18 L. T. Saldin, M. C. Cramer, S. S. Velankar, L. J. White and S. F. Badylak, Acta Biomater., 2017, 49, 1–15.
19 E. A. Kiyotake, E. C. Beck and M. S. Detamore, Ann. N. Y. Acad. Sci., 2016, 1383, 139–159.
20 H. V Almeida, A. D. Dikina, K. J. Mulhall, F. J. O. Brien, E. Alsberg and D. J. Kelly, ACS Biomater. Sci. Eng., 2017, 3, 1075–1082.
21 I. Gadjanski, K. Spiller and G. Vunjak-Novakovic, Stem Cell Rev. Reports, 2012, 8, 863–881.
22 R. Cai, T. Nakamoto, N. Kawazoe and G. Chen, Biomaterials, 2015, 52, 199–207.
23 J. Liu, C. Yu, Y. Chen, H. Cai, H. Lin, Y. Sun, J. Liang, Q. Wang, Y. Fan and X. Zhang, J. Mater. Chem. B, 2017, 5, 9130–9140.
24 G. Ragetly, D. J. Griffon and Y. S. Chung, Acta Biomater., 2010, 6, 3988–3997.
25 N. H. Dormer, M. Singh, L. Wang, C. J. Berkland and M. S. Detamore, Ann. Biomed. Eng., 2010, 38, 2167–2182.
26 W. L. Grayson, F. Zhao, R. Izadpanah, B. Bunnell and T. Ma, J. Cell. Physiol., 2006, 207, 331–339.
27 H. L. Fermor, S. W. D. McLure, S. D. Taylor, S. L. Russell, S. Williams, J. Fisher and E. Ingham, Biomed. Mater. Eng., 2015, 25, 381–395.
28 L. Xing, Y. Jiang, J. Gui, Y. Lu, F. Gao, Y. Xu and Y. Xu, Knee Surgery, Sport. Traumatol. Arthrosc., 2013, 21, 1770–1776.
29 C. Bougault, L. Cueru, J. Bariller, M. Malbouyres, A. Paumier, A. Aszodi, Y. Berthier, F. Mallein-Gerin and A. M. Trunfio-Sfarghiu, J. Biomech., 2013, 46, 1633–1640.
30 K. E. M. Benders, P. R. van Weeren, S. F. Badylak, D. B. F. Saris, W. J. A. Dhert and J. Malda, Trends Biotechnol., 2013, 31, 169–176.
31 F. Pati, J. Jang, D.-H. Ha, S. Won Kim, J.-W. Rhie, J.-H. Shim, D.-H. Kim and D.-W. Cho, Nat. Commun., 2014, 5, 3935.
32 J. Kundu, A. Michaelson, K. Talbot, P. Baranov, M. J. Young and R. L. Carrier, Acta Biomater., 2016, 31, 61–70.

33 Y. Y. Li, T. H. Choy, F. C. Ho and P. B. Chan, Biomaterials, 2015, 52, 208–220.
34 N. J. Hallab, K. J. Bundy, K. O'Connor, R. L. Moses and J. J. Jacobs, Tissue Eng., 2001, 7, 55–71.
35 K. Chaipinyo, B. W. Oakes and M.-P. I. Van Damme, J. Orthop. Res., 2004, 22, 446–55.
36 C. Tang, C. Jin, Y. Xu, B. Wei and L. Wang, Tissue Eng. Part A, 2016, 22, 222–32.
37 L. Zhang, T. Yuan, L. Guo and X. Zhang, J. Biomed. Mater. Res. - Part A, 2012, 100 A, 2717–2725.
38 A. Higuchi, Q. D. Ling, S. T. Hsu and A. Umezawa, Chem. Rev., 2012, 112, 4507–4540.
39 J. P. Vacanti and R. Langer, Lancet, 1999, 354, S32–S34.
40 A. Svensson, E. Nicklasson, T. Harrah, B. Panilaitis, D. L. Kaplan, M. Brittberg and P. Gatenholm, Biomaterials, 2005, 26, 419–431.
41 S. Kang, J. B. Park, T. J. Lee, S. Ryu, S. H. Bhang, W. G. La, M. K. Noh, B. H. Hong and B. S. Kim, Carbon N. Y., 2015, 83, 162–172.
42 B. Cao, R. Peng, Z. Li and J. Ding, Biomaterials, 2014, 35, 6871–6881.
43 N. Mahmoudifar and P. M. Doran, Trends Biotechnol., 2012, 30, 166–176.
44 D. Ollitrault, F. Legendre, C. Drougard, M. Briand, H. Benateau, D. Goux, H. Chajra, L. Poulain, D. Hartmann, D. Vivien, V. Shridhar, A. Baldi, F. Mallein-Gerin, K. Boumediene, M. Demoor and P. Galera, Tissue Eng. Part C. Methods, 2014, 00, 1–15.
45 A. Sterodimas and J. de Faria, Aesthet. Surg. J., 2013, 33, 283–9.
46 K. Kim, J. Lam, S. Lu, P. P. Spicer, A. Lueckgen, Y. Tabata, M. E. Wong, J. A. Jansen, A. G. Mikos and F. K. Kasper, J. Control. Release, 2013, 168, 166–178.
47 L. A. Fortier, J. U. Barker, E. J. Strauss, T. M. McCarrel and B. J. Cole, Clin. Orthop. Relat. Res., 2011, 469, 2706–2715.
48 R. A. Thibault, A. G. Mikos and F. K. Kasper, Biomacromolecules, 2011, 12, 4204–4212.
49 S. Ravindran, M. Kotecha, C. C. Huang, A. Ye, P. Pothirajan, Z. Yin, R. Magin and A. George, Biomaterials, 2015, 71, 58–70.
50 J. B. Tang, Y. F. Wu, Y. Cao, C. H. Chen, Y. L. Zhou, B. Avanessian, M. Shimada, X. T. Wang and P. Y. Liu, Sci. Rep., 2016, 6, 1–12.
51 C. J. Li, V. Madhu, G. Balian, A. S. Dighe and Q. Cui, J. Cell. Physiol., 2015, 230, 2671–2682.
52 J. Liu, H. Lin, X. Li, Y. Fan and X. Zhang, RSC Adv., 2015, 5, 54446–54453.
53 C. Yu, J. Liu, G. Lu, Y. Xie, Y. Sun, J. Liang, Y. Fan, X. Zhang and Q. Wang, J. Mater. Chem. B, 2018, 5164–5173.
54 Y. Sun, L. Yan, S. Chen and M. Pei, Acta Biomater., 2018, 74, 56–73.
55 H.W. Cheng, Y.K. Tsui, K. M. C. Cheung, D. Chan and B. P. Chan, Tissue Eng. Part C. Methods, 2009, 15, 697–706.
56 S. K. Brusnahan, T. R. McGuire, J. D. Jackson, J. T. Lane, K. L. Garvin, B. J. O'Kane, A. M. Berger, S. R. Tuljapurkar, M. A. Kessinger and J. G. Sharp, Mech. Ageing Dev., 2010, 131, 718–722.
57 G. Kasper, L. Mao, S. Geissler, A. Draycheva, J. Trippens, J. Kühnisch, M. Tschirschmann, K. Kaspar, C. Perka, G. N. Duda and J. Klose, Stem Cells, 2009, 27, 1288–1297.

Bionic Cartilage Acellular Matrix Microspheres as scaffold for engineering cartilage

Keyword： microspheres, extracellular matrix, decellularization, chondrogenesis, tissue engineering

Jun Liu, Xiuyu Wang, Gonggong Lu, James Z. Tang, Yonghui Wang, Boqing Zhang, Yong Sun, Hai Lin, Qiguang Wang*, Jie Liang, Yujiang Fan*, Xingdong Zhang

Bionic cartilage acellular matrix microsphere (BCAMM) made from decelluarized bionic cartilage microspheres (BCM)